STATUS OF ELECTRON-CLOUD BUILD-UP SIMULATIONS FOR THE MAIN INJECTOR*

M. A. Furman,† LBNL, Berkeley, CA 94720-8211, USA
I. Kourbanis and R. M. Zwaska, Fermilab, Batavia, IL 60510, USA

INTRODUCTION

An upgrade to the MI is being considered that would increase the bunch intensity N_b from the present $\sim 1 \times 10^{11}$ to 3×10^{11}, corresponding to a total pulse intensity $N_{\rm tot} = 16.4 \times 10^{13}$, in order to generate intense beams for the neutrino program [1]. Such an increase in beam intensity would place the MI in a parameter regime where other storage rings have seen a significant EC effect. Motivated by this concern, efforts have been undertaken over the recent past to measure [2–5] and simulate [6–15] the magnitude of the effect and to assess its operational implications on the proposed upgrade.

We report here a summary of simulation results obtained with the code POSINST [16, 17], and certain benchmarks against measurements. Unless stated otherwise, the simulation parameters used are shown in Tab. 1. Some of these represent a slightly simplified version of the MI operation.

DEPENDENCE ON SEY

During 2006 an RFA-type electron detector was installed in a field-free straight section of the MI and was used to measure the electron flux J_e incident on the RFA for various bunch intensities N_b and fill patterns [2–5]. Fig. 1 of Ref. [11] summarizes the measurements.

The primary unknown variable in the EC intensity build-up is the peak value of the secondary electron yield (SEY) $\delta_{\rm max}$. By fixing other variables and then running simulations for various assumed values of $\delta_{\rm max}$, we were able to fit the measurements [11], as shown in Fig. 1, obtaining $1.25 \lesssim \delta_{\rm max} \lesssim 1.30$. The close clustering of the solutions, which were obtained for rather varied beam conditions, indicates consistency in the simulation model and the measurements. For all other results presented in this article we assumed $\delta_{\rm max} = 1.3$.

The EC number density n_e inferred from these measurements is sufficiently low that it is not expected to cause significant detrimental effects on the beams used in the measurements. This absence of an effect is, indeed, consistent with observations.

DEPENDENCE ON N_b

The dependence of n_e on N_b is shown in Figs. 2-3, where n_e represents the one-turn average of the electron density in the entire section being simulated (the local density in the neighborhood of the beam is substantially higher) [12–14]. Also shown is the average electron-wall impact energy E_0.

Table 1: Selected MI parameters used in most simulations.

Ring and beam	
Ring circumference	$C = 3319.419$ m
RF frequency	$f_{\rm RF} = 52.809$ MHz
Harmonic number	$h = 588$
Beam fill pattern	500 full + 88 empty
Beam energy	$E_b = 8.9 - 120$ GeV
Bunch profile	3D gaussian
Transv. RMS bunch sizes at 8.9 GeV †	$(\sigma_x, \sigma_y) = (2.3, 2.8)$ mm
RMS bunch length σ_z	see Fig. 4
Pipe cross sect. at RFA	round
Pipe radius at RFA	$a = 7.3$ cm
Pipe cross sect. at dipole	elliptical
Pipe semiaxes at dipole	$(a, b) = (6.15, 2.45)$ cm
Dipole bending field	0.0115 T/(GeV/c)
Secondary e⁻ parameters	
Peak SEY	$\delta_{\rm max} = 1.2 - 1.4$
Energy at $\delta_{\rm max}$	$E_{\rm max} = 292.6$ eV
SEY at 0 energy	$\delta(0) = 0.2438 \times \delta_{\rm max}$

† At other energies, σ_x and σ_y were assumed to scale as $\gamma^{-1/2}$.

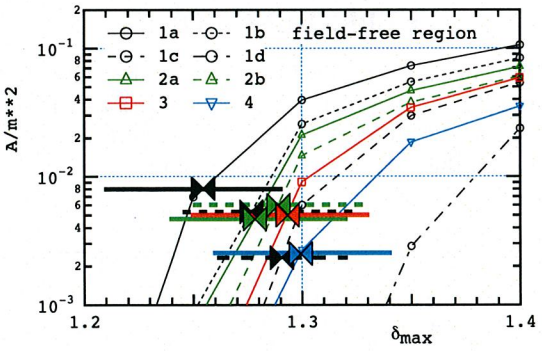

Figure 1: Simulated electron flux J_e vs. $\delta_{\rm max}$ (curves) and RFA measurements (thick horizontal lines) for the respective fill patterns. The bowties indicate the intersections of the measurements with the simulations for each case [11].

*Work supported by the US DOE under contracts DE-AC02-05CH11231 (LBNL) and DE-AC02-07CH11359 (FNAL).

† mafurman@lbl.gov

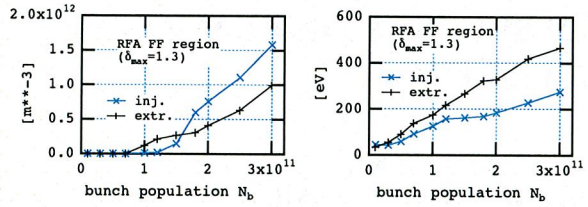

Figure 2: Average n_e and E_0 in the field-free region containing the RFA, at injection and extraction E_b.

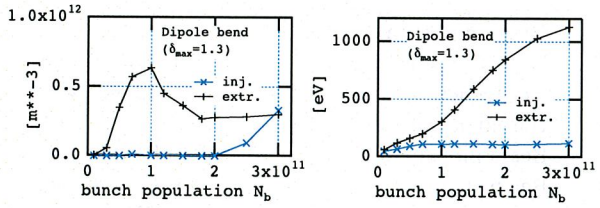

Figure 3: Average n_e and E_0 in a dipole bending magnet at injection and extraction E_b.

DEPENDENCE ON E_b

The primary dependence of the EC build-up on beam energy E_b is through the bunch length, which varies substantially as E_b ramps from 8.9 GeV to 120 GeV, as seen in Fig. 4. The simulated density n_e vs. E_b is shown Figs. 5-6 for two selected values of N_b. There is appreciable variation of n_e only near transition energy, where σ_z is smallest, as expected.

DEPENDENCE ON $f_{\rm RF}$

We compared [12] the EC density for the actual RF frequency $f_{\rm RF} = 53$ MHz ($h = 588$) against a hypothetical value of 212 MHz ($h = 4 \times 588 = 2352$). For the purposes of this exercise we assumed, for $f_{\rm RF} = 53$ MHz,

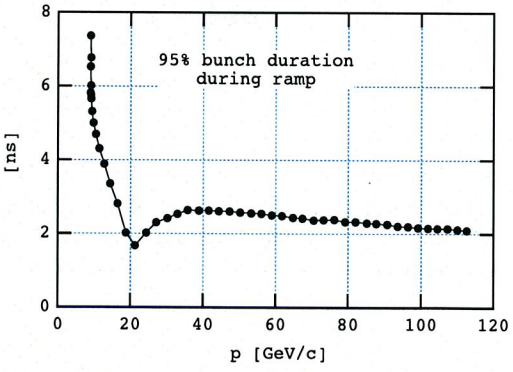

Figure 4: Measured 95% bunch length during the ramp. Transition is crossed just above 20 GeV/c.

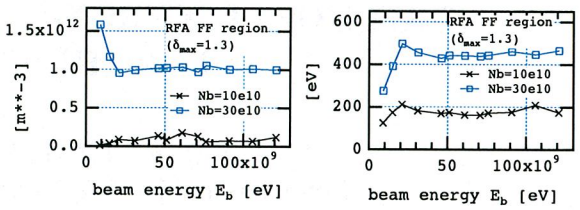

Figure 5: Average n_e and E_0 vs. E_b in the RFA field-free region for two values of N_b.

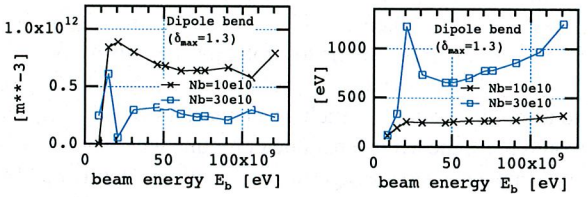

Figure 6: Average n_e and E_0 vs. E_b in a dipole bending magnet for two values of N_b.

a fill pattern consisting of 548 consecutive filled buckets, each with N_b protons and RMS bunch length σ_z, plus 40 empty buckets. For 212 MHz we assumed 2192 filled buckets, each with $N_b/4$ protons and RMS bunch length $\sigma_z/4$, plus 160 empty buckets. All other quantities were kept fixed. The total number of protons per pulse in either case is $N_{\rm tot} = 548 \times N_b = 2192 \times (N_b/4)$. Results are shown in Fig. 7.

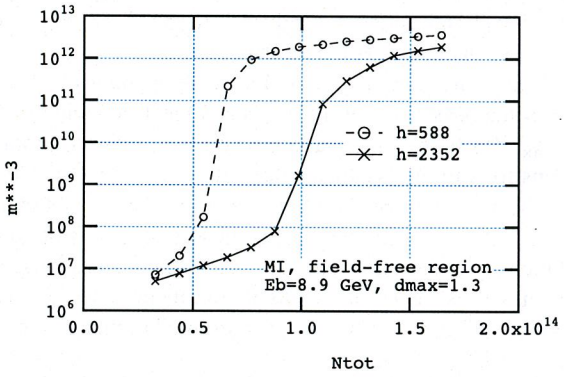

Figure 7: Average n_e vs. $N_{\rm tot}$ in the RFA field-free region for $f_{\rm RF} = 53$ and 212 MHz at injection E_b.

DISCUSSION

Having simulated various current operational scenarios and compared our results against RFA measurements, we have obtained a reasonably consistent picture indicating $\delta_{\rm max} \sim 1.3$, assuming $E_{\rm max} = 293$ eV. Although this value for $E_{\rm max}$ is realistic, we do not have evidence that it is the actual value for the MI vacuum chamber (a typi-

cal range for $E_{\max}$ is 250–350 eV). It is generally possible to trade off, to some extent, $\delta_{\max}$ and $E_{\max}$ for each other in any given fit to the data. Pinning down both parameters requires a broader set of simultaneous fits than we have carried out, and this exercise remains to be done.

Extrapolating our simulations to higher beam intensities, we predict a significant increase of the electron density n_e in field-free regions. For these, n_e exhibits a threshold behavior in N_b, with approximately linear dependence on $(N_b - N_{b,\mathrm{th}})$ above the threshold $N_{b,\mathrm{th}}$. For a dipole bending magnet there is no indication of threshold behavior in N_b: n_e increases rather strongly, and non-monotonically, for N_b above $\sim 2 \times 10^{10}$, and further changes are E_b-dependent. At the design goal, $N_{\mathrm{tot}} = 16.4 \times 10^{13}$, we estimate the time-averaged, volume-averaged n_e in the range $(0.1 - 1) \times 10^{12}$ m^{-3} (the density in the neighborhood of the beam is substantially higher). The peak exhibited by n_e at $N_b \sim 1 \times 10^{11}$ in a dipole can be explained from the E_0 data: when $N_b \simeq 1 \times 10^{11}$, E_0 crosses 300 eV, the assumed value for the location of the SEY peak. The actual value of N_b where n_e peaks depends on the actual value of $E_{\max}$. The dependence of E_0 on N_b, however, does not explain all simulation trends; this issue remains to be better understood. In particular, we do not yet have an explanation for the increase of n_e at $N_b \lesssim 3 \times 10^{11}$ at injection E_b in a dipole magnet.

The dependence of n_e on E_b is generally mild except near transition energy, given that the bunch length has strongest variation about this energy. This translates into strong variation of the strength of the beam-electron kick, hence into strong variation of E_0, hence of the effective SEY, hence of n_e. For E_0 significantly larger than $E_{\max}$ the effective SEY is smaller that for $E_0 \sim E_{\max}$. This accounts for the reversal in the dependence of n_e for the two selected values of N_b when comparing the field-free region and the dipole magnet. The mild sensitivity of the EC to E_b is consistent with recent measurements via the microwave dispersion technique [18], but not with RFA measurements. These latter show a rather strong dependence on E_b, typically peaking at $E_b \sim 60$ GeV. This issue remains to be clarified.

Going to a hypothetical f_{RF} four times larger than the present 53 MHz, with 4 times smaller bunch population, leads to a threshold of the EC build-up ~ 2 times higher in N_{tot} in a field-free region relative to the 53 MHz case. Above threshold, including the design goal of $N_{\mathrm{tot}} = 16.4 \times 10^{13}$, the density is $\sim 2 - 4$ times lower for the higher f_{RF} than for the lower. Preliminary simulations for a dipole bending magnet, however, do not show such a beneficial trend at the higher f_{RF}, and remain to be properly analyzed and understood.

Our overall experience with simulations of proton storage rings, including the MI, consistently show that the vacuum chamber SEY is the main variable that determines n_e and hence the severity of all EC-related effects. The surest way to decrease these effects, therefore, is to decrease the SEY of the vacuum chamber by means of low-emission coatings, grooved surfaces, clearing electrodes, appropriate magnetic fields, etc.

We have checked the numerical stability of our simulation results against computational parameters such as the integration time step, space-charge grid size and number of macroparticles, but not in all combinations. While with have confidence in our results, a final check for any given specific set of physical parameters check remains to be carry out. In any case, a clear qualitative picture of the EC build up in the MI field-free regions and dipole bending magnets is emerging.

Initial simulations of the effects from the EC on the beam have been carried out [15]. These calculations indicate a threshold $n_e \sim 10^{12}$ m^{-3} for significant emittance growth, which is in the range of our EC density estimates. Therefore, it is important to pursue such investigations further.

Recent simulations [19] of the EC build-up for the proposed PS2 storage ring at CERN show results remarkably similar to those summarized here for the MI. Therefore, a program of benchmarks will benefit the beam dynamics studies in both machines.

ACKNOWLEDGMENTS

We are grateful to C. Celata, G. Penn, K. Sonnad, J.-L. Vay and M. Venturini for discussions.

REFERENCES

[1] Proton Driver Study. II. (Part 1, ch. 13), FERMILAB-TM-2169 (G. W. Foster, W. Chou and E. Malamud, eds.), May 2002.

[2] R. Zwaska, Proc. ECLOUD07.

[3] I. Kourbanis, "e-Cloud MI Measurements", 26 Aug. 2007.

[4] R. Zwaska, Proc. HB2008.

[5] X. Zhang et. al., Proc. PAC07, paper THPAN117.

[6] M. A. Furman, LBNL-57634/CBP-Note-712/FERMILAB-PUB-05-258-AD and New J. Phys. **8** (2006) 279.

[7] M. A. Furman, Proc. HB2006.

[8] M. A. Furman, CBP-Technote-364/FERMILAB-TM-2369-AD.

[9] M. A. Furman, CBP Technote-367.

[10] M. A. Furman, Proc. ECLOUD07.

[11] M. A. Furman, LBNL-1402E/CBP Tech Note 387 and Proc. HB2008.

[12] M. A. Furman, CBP-Technote-386.

[13] M. A. Furman, CBP-Technote-392.

[14] M. A. Furman, CBP-Technote-390.

[15] K. G. Sonnad, M. A. Furman and J.-L. Vay, LBNL-767E.

[16] M. A. Furman and G. R. Lambertson, Proc. MBI-97, p. 170.

[17] M. A. Furman and M. T. F. Pivi, PRST-AB **5** 124404 (2003).

[18] N. Eddy et. al., these proceedings.

[19] M. A. Furman, LARP-CM12.